MITIGATING THE PERIODIC RESONANCE CROSSING IN HIGH-INTENSITY BUNCHES BY MULTI-RF

G. Franchetti[1,2,3], S. Albright[4], F. Asvesta[4], H. Bartosik[4], T. Prebibaj[4]
[1]GSI Helmholtzzentrum für Schwerionenforschung GmbH, Darmstadt, Germany
[2]Goethe University Frankfurt, Frankfurt, Germany
[3]Helmholtz Research Academy Hesse for FAIR, Frankfurt, Germany
[4]CERN, Geneva, Switzerland

Abstract

Periodic resonance crossing driven by space charge in bunched beams leads to slow diffusion over hundreds of synchrotron oscillations, making emittance growth and beam loss difficult to control and hard to describe theoretically. Its pseudo-stochastic nature means reliable predictions typically require full simulations. Mitigation methods such as resonance compensation or space-charge compensation are complex and highly dependent on detailed machine conditions. Here, an alternative approach is proposed: shaping the longitudinal bunch profile using a suitable combination of RF harmonics to reduce the effectiveness of periodic crossings. First experimental studies at the CERN PS Booster show promising results, suggesting this as a viable new direction.

PERIODIC RESONANCE CROSSING IN HIGH INTENSITY BUNCHES

The rise of new operational regimes in particle accelerators has introduced significant challenges for recent projects [1, 2]. For example, the FAIR project [1] involves long-term storage of high-intensity bunched beams over hundreds of synchrotron oscillations. During this time, particles repeatedly traverse regions of varying longitudinal density, coupling the transverse space-charge tune shift to their longitudinal motion. This becomes critical when the tune spread overlaps a lattice resonance, causing resonance islands to vary with longitudinal position and move in the transverse plane. As particles cross these moving islands, their invariant $J_{x/y} = 2\epsilon_{x/y}$ can change: fast crossings produce random-like kicks (scattering), while slow crossings may trap particles. This leads to transverse diffusion, halo formation, and eventual beam loss if the halo exceeds machine acceptance. Experiments at GSI (SIS18) [3] and CERN (PS, SPS) [4, 5] confirm this mechanism. Modeling this process is challenging because the scattering is pseudo-random [6] and nonlinear, leading to diffusion that depends on resonance properties, additional nonlinearities (e.g., amplitude-dependent detuning), and the synchrotron motion speed.

Mitigation Approaches

The impact of resonance islands on particle dynamics depends on resonance strength. Weak resonances cause weaker scattering during periodic crossings, leading to slower halo formation and beam loss—making mitigation more feasible. This was demonstrated at SIS18 [7], where partial compensation of a third-order resonance reduced emittance growth and losses. However, resonance compensation is challenging. It is typically based on single-particle estimates of resonant driving terms [8], whereas in reality the optics are modified by space charge [9, 10]. As a result, compensation varies along the bunch and may become less effective, especially when multiple resonances overlap with the incoherent tune spread. An alternative approach targets the space-charge effect directly using electron lenses, which generate opposing fields to compensate amplitude-dependent detuning. This replaces the continuous space-charge force with localized, longitudinally modulated lenses matched to the bunch profile [11, 12]. Multiple lenses help avoid introducing additional resonances or perturbing the optics. Another strategy, explored at IOTA (FNAL) [13], uses integrable optics based on the McMillan concept [14, 15]. Here, specially designed magnetic fields intrinsically mitigate space-charge effects and stabilize beam dynamics. Ongoing experiments are investigating its effectiveness for periodic resonance crossing in intense proton beams.

NOVEL APPROACH

Here, a different mitigation strategy is proposed: instead of targeting the resonance itself (as in resonance compensation), the detuning (e-lenses), or resonance formation (integrable optics), the goal is to reduce the scattering process directly. This is done by controlling the speed at which instantaneous resonance islands cross particle orbits. If the crossing is slow—so the phase advance in the frame island is many multiples of 2π during one synchrotron oscillation—particles can become trapped. If the crossing is fast, the interaction is much weaker. The next discussion focuses on a 1D resonance of the form $n_x Q_x = N$. The speed of an island crossing is the composition of the speed of the longitudinal motion $\Delta z/\Delta n$, with n the turn number, with the dependence of the instantaneous fixed point $(x_{\rm fp}, x'_{\rm fp})$ on the longitudinal position of the particle z. For an axi-symmetric transverse Gaussian distribution, considering a particle with $\epsilon_y = 0$, the dependence of the incoherent space charge tuneshift is $\Delta Q_{x,\rm sc}(\epsilon_x, z) \simeq \Delta Q_{x0,\rm sc}(z)/[1 + \epsilon_x/(4E_x)]$, with E_x the horizontal rms emittance, and $\Delta Q_{x0,\rm sc}(z)$ the maximum transverse incoherent space charge tuneshift at location z (where the particle we consider is). The location of the fixed points is approximately determined by the resonance condition $\Delta Q_{x,\rm sc}(\epsilon_{x,\rm fp}, z) \simeq Q_{x,r} - Q_{x0}$, with $Q_{x,r}$ the

tune at which the resonance is located, and Q_{x0} the bare machine tune. The term $\epsilon_{x,\mathrm{fp}}$ refers to the invariant of the instantaneous fixed point. As the bunch aspect ratio $\sigma_{x/y}/\sigma_z \ll 1$ we have that $\Delta Q_{x0,\mathrm{sc}}(z) \propto \lambda(z)$, with $\lambda(z)$ the longitudinal charge line density, hence the speed of migration of the fixed point implicitly obtained from $\Delta[\Delta Q_{x,\mathrm{sc}}(\epsilon_{x,\mathrm{fp}}, z)]/\Delta n_t = 0$, in terms of $\epsilon_{x,\mathrm{fp}}$, reads

$$\frac{\Delta\epsilon_{x,\mathrm{fp}}}{\Delta n_t} \simeq 4E_x\left(1+\frac{\epsilon_{x,\mathrm{fp}}}{4E_x}\right)\frac{1}{\lambda(z)}\frac{d\lambda(z)}{dz}\frac{\Delta z}{\Delta n_t}\,, \qquad (1)$$

where n_t is the turn number. This relation shows that the speed of motion of the fixed points, which is $\propto \sqrt{|\Delta\epsilon_{x,\mathrm{fp}}/\Delta n_t|}$, depends on the speed of the synchrotron motion $\Delta z/\Delta n_t$ and on the derivative of the longitudinal charge line density $\lambda(z)$.

As the longitudinal distribution can be manipulated via proper RF gymnastics or a combination of RF harmonics, we may act on $\Delta\epsilon_{x,\mathrm{fp}}/\Delta n_t$ by properly shaping the longitudinal particle distribution $\lambda(z)$ to alter the speed of resonance crossing and thus make the scattering process less effective. Equation (1) suggests that the relevant properties of the longitudinal distribution and the RF, are: P1) existence of a central region where $d\lambda(z)/dz \simeq 0$, hence particles moving through it are not crossed by resonance islands; P2) the regions with $d\lambda(z)/dz \neq 0$ should have very large $(d\lambda(z)/dz)(\Delta z/\Delta n_t)$, as in this case the fixed points move very fast, making the scattering process less effective. The properties P1 and P2 seems to conflict with each other, and their implementation is the challenge. Next, we discuss a dedicated RF bucket and its matched longitudinal distribution in relation with the property P1.

We consider a composition of several even harmonics in an RF system to build a well-shaped RF potential well. The RF force F acting on a particle is the result of the composition of the following RF harmonics

$$F = \sum_{q=1}^{n} V_q \sin(q\frac{\pi}{z_b}z + q\pi),$$

with $V_q = V_{\max}\frac{1}{2^{2n-1}}\binom{2n}{n+q}q\frac{\pi}{z_b}$, where z_b is the half bucket length and q is the harmonic number. This force creates the RF potential $V(z) = V_{\max}\sin^{2n}\left(\frac{\pi}{2}\frac{z}{z_b}\right)$. An example of the scaled force (red curve) and of the scaled potential (blue curve) for $n = 1$, and $n = 10$ is shown in Fig. 1 top. This picture shows clearly the property of this composition of harmonics: with the increase of n, the potential well (blue curve) becomes flatter and flatter, converging towards a barrier bucket, while the force exerted on the particles becomes very small in the center of the bucket. The longitudinal dynamics is given by the equation $z'' + \partial_z V(z) = 0$, and defining $p_z = z'$, the Hamiltonian of the system reads $H = p_z^2/2 + V(z)$. The orbits in the phase space are the level curves of this Hamiltonian shown in Fig. 1 bottom to highlight their shape. The special form of the potential affects the amplitude-dependent synchrotron tune, shown in terms of synchrotron period in Fig. 2 (left). The synchrotron period

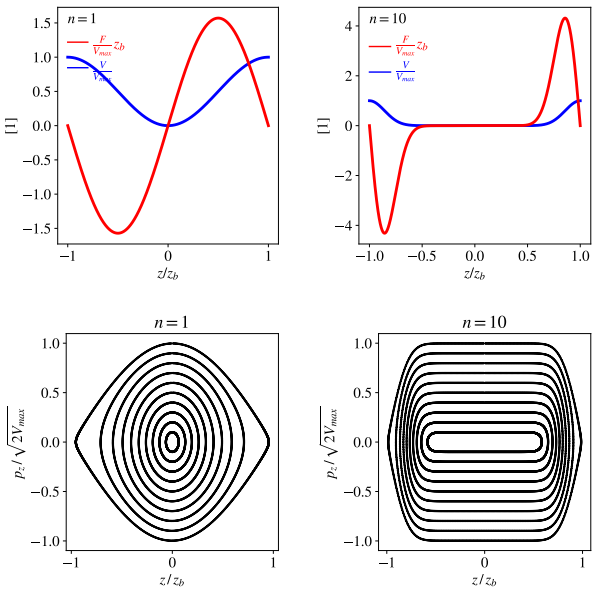

Figure 1: Top: Example of the normalized RF potential and RF force as created by one harmonic (left), and 10 (even) harmonics (right). Bottom: Corresponding orbits in the normalized phase space.

is normalized with the corresponding period S_1 in the center of a one-harmonic bucket. The picture shows, in terms of $w = H/V_{\max}$, that for $n = 1$ and $w \to 0$ the synchrotron period is equal to the standard one. The black curve also shows that the period diverges as $w \to 1$, which corresponds to the dynamics at the separatrix. Note the completely different dependence for $n > 1$, where the period diverges for $w \to 0$ as well as for $w \to 1$. This feature arises because the composition of harmonics produces a potential well with second derivative zero at the bucket center ($w = 0$). This feature is also highlighted by Fig. 2 (right), which shows the maximum oscillation amplitude of the particles in the bucket. For larger n and same w, a particle oscillates on a larger region, again showing that in the bucket center, there is no acting force. This feature is relevant in Eq. (1) as the speed of fixed point migration is also determined by $\Delta z/\Delta n_t$. We next investigate for this general type of RF bucket whether the matched distribution is proper to satisfy the property P1.

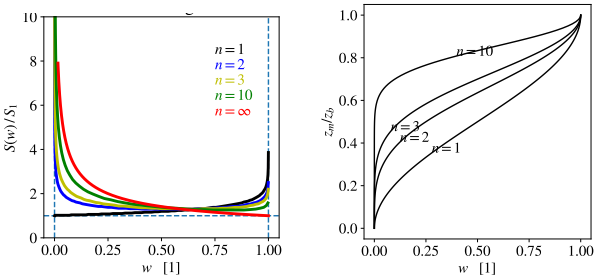

Figure 2: Left: Normalized synchrotron tune as function of $w = H/V_{max}$ for several harmonics composition. Right: Maximum oscillation amplitude z_m according to orbits and harmonics used.

We consider the matched parabolic particle distribution, here not affected by longitudinal space charge or collective fields, $\rho(z,z') \propto \sqrt{1-H/(\sigma V_{\max})}$. The quantity σ is a filling factor of the nonlinear RF bucket. The projection on the z axis yields

$$\lambda(\tilde{z}) = \frac{N_0}{z_b \Lambda_n(\sigma)} \left[1 - \frac{1}{\sigma^2} \sin^{2n}\left(\frac{\pi}{2}\tilde{z}\right)\right], \qquad (2)$$

with $\tilde{z} = z/z_b$ and $-\tilde{z}_l < \tilde{z} < \tilde{z}_l$, and $\Lambda_n(\sigma)$ a normalization factor to ensure that $\int_{-\tilde{z}_l}^{\tilde{z}_l} \lambda(\tilde{z})dz = 1$. The distribution edge $\tilde{z}_l$ is the solution of the equation $\sigma = \sin^n\left(\frac{\pi}{2}\tilde{z}_l\right)$. Figure 3 shows an example of beam distribution for $n = 10$, and occupation $\sigma = 0.4$, with the normalized phase space distribution (left) and its projection on z (right). The magenta curve is the theoretical prediction of Eq. (2). This distribution satisfies P1. Next, we investigate the consequences of

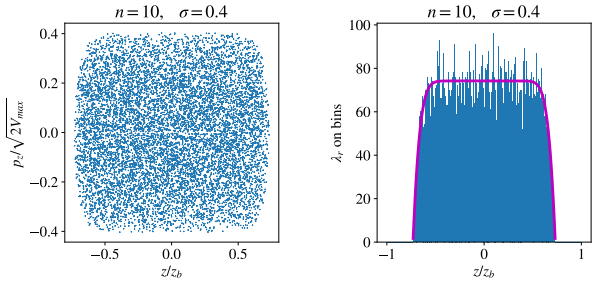

Figure 3: Left: Normalized matched particle distribution, for $n = 10$, and $\sigma = 0.4$. Right: corresponding longitudinal particle distribution (blue histogram), and the theoretical curve (magenta).

the property P1. To this purpose we compute, as figure of merit, the fraction of particles $N_{\rm nc}/N_0$, which always remain in the flat region of the bunch, hence that are not subject to the periodic resonance crossing phenomenon. As the larger $\lambda(z)$ is found at $z = 0$, we consider the flat region of the bunch as $-\tilde{z}_f < \tilde{z} < \tilde{z}_f$ with $\tilde{z}_f$ the edge of flatness defined as $\beta = 1 - \lambda(z_f)/\lambda(0)$, with β the criterion for assessing the region of flatness. All particles that oscillate in the flat region will not be periodically crossed by the moving islands. Hence, it would be desirable that for $n \to \infty$ we had $N_{\rm nc}/N_0 \to 1$. Figure 4 shows the number of particles in the flat region as a function of n, β, σ. The picture clearly shows a weak sensitivity to the occupation number σ, whereas it is much stronger to the criterion of flatness β. The curves pattern also show that the fraction of particles in the flat region does not grow to 100 % increasing n, but rather converges to an asymptotic limit. This surprising finding stems form the matching condition. In fact, once β is set then w_f is set, and by increasing n, the edge of flatness $\tilde{z}_f$ move towards the edge of the bucket, while at the same time the height of the orbit passing through $(\tilde{z}_f, 0)$ remain the same $p_{z,m} = \sqrt{2w_f V_{\max}}$, and the full orbit becomes more and more rectangular, hence creating the asymptotic pattern. Note that Fig. 4 gives a very conservative estimate; in fact, there are more particles that travel through the varying $\lambda(z)$,

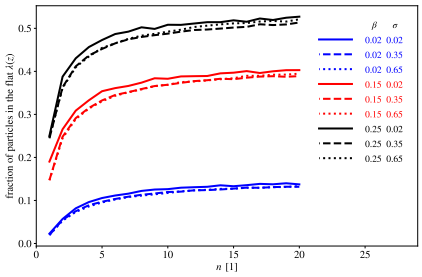

Figure 4: Fraction of particles that remain in the flat region (defined by β) of the longitudinal particle density. It is also investigated the dependence on the filling of the bucket (defined by σ).

but necessarily do not cross the resonance. Assessing this amount requires a full computation of the transverse incoherent space charge tuneshift and its dependences from the transverse oscillation amplitudes $(x_m, y_m), z$, and verifying when, for a given Q_{x0} and $Q_{x,r}$, particles never cross the resonance.

Following these preliminary results, we experimentally investigated the beam response to a multi-harmonics RF in a few cases. The experiment have been carried out at the CERN-PSB, the 3rd order resonance $3Q_y = 13$ has been intentionally excited, and a bunched beam with $\Delta Q_{\rm sc} \simeq 0.05$ was stored for ~1 s. Figure 5 (left) shows the emittance response employing a one-harmonics bucket for a tune scan in the region of the stop-band. The emittance response fol-

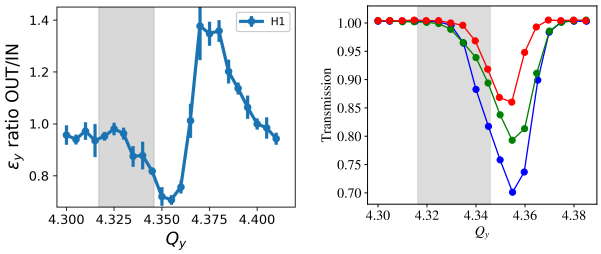

Figure 5: The gray area is the resonance stop-band. Left: emittance growth due to the periodic resonance crossing; Right: beam loss for space charge equivalent bunched beams.

lows the same pattern observed in previous studies [1,4,5]. At the time of the measurement, only odd harmonics were available, which nevertheless have been used to approximate the ideal RF potential. Figure 5 (right) shows the beam survival when 1st (blue), odd harmonics up to 3rd (green), and up to the 11th (red) harmonics are used to confine bunches with a similar space-charge tune shift (adapting the bunch population accordingly).

CONCLUSIONS

This preliminary result of improved beam transmissions when deploying a multiharmonic RF system to resemble a barrier bucket is very encouraging, and further endorses more precise experimental investigations with an RF bucket composed by even harmonics only.

REFERENCES

[1] P. Spiller and G. Franchetti, "The FAIR accelerator project at GSI", *Nucl. Instrum. Methods Phys. Res. A*, vol. 561, no. 2, pp. 305–309, 2006. doi:10.1016/j.nima.2006.01.043

[2] G. Rumolo, "CERN LIU project: beam dynamics aspects and solutions", *CERN Yellow Rep. School Proc.*, vol. 3, p. 2141, 2024. doi:10.23730/CYRSP-2024-003.2141

[3] G. Franchetti *et al.*, "Experiment on space charge driven nonlinear resonance crossing in an ion synchrotron", *Phys. Rev. Spec. Top. Accel. Beams*, vol. 13, p. 114203, 2010. doi:10.1103/PhysRevSTAB.13.114203

[4] G. Franchetti, I. Hofmann, M. Giovannozzi, M. Martini, and E. Metral, "Space charge and octupole driven resonance trapping observed at the CERN Proton Synchrotron", *Phys. Rev. Spec. Top. Accel. Beams*, vol. 6, no. 12, p. 124201, 2003. doi:10.1103/PhysRevSTAB.6.124201

[5] G. Franchetti, S. Gilardoni, A. Huschauer, F. Schmidt, and R. Wasef, "Space charge effects on the third order coupled resonance", *Phys. Rev. Accel. Beams*, vol. 20, no. 8, p. 081006, Aug. 2017. doi:10.1103/PhysRevAccelBeams.20.081006

[6] A. I. Neishtadt, "Passage through a separatrix in a resonance problem with a slowly-varying parameter", *J. Appl. Math. Mech.*, vol. 39, no. 4, pp. 594–605, 1975. doi:10.1016/0021-8928(75)90060-X

[7] G. Franchetti *et al.*, "Resonance Compensation for High Intensity Bunched Beams", in *Proc. IPAC'15*, Richmond, VA, USA, May 2015, pp. 159–161. doi:10.18429/JACoW-IPAC2015-MOPWA028

[8] G. Guignard, "A general treatment of resonances in accelerators", CERN, Geneva, Switzerland, Rep. CERN-78-11, 1978.

[9] G. Franchetti, "Space Charge in Circular Machines", *CERN Yellow Rep. School Proc.*, vol. 3, p. 353, 2017. doi:10.23730/CYRSP-2017-003.353

[10] C. Guo, J. Liu, J. C. Yang, and R. H. Zhu, "Simulation studies on compensation for incoherent magnet error driven half-integer and 3rd-order resonances with space charge in hiaf-bring", *Nucl. Instrum. Methods Phys. Res. A*, vol. 1082, p. 171003, 2026. doi:10.1016/j.nima.2025.171003

[11] A. Oeftiger and O. Boine-Frankenheim, "Pulsed Electron Lenses for Space Charge Mitigation", *Phys. Rev. Lett.*, vol. 132, no. 17, p. 175001, 2024. doi:10.1103/PhysRevLett.132.175001

[12] K. Schulte-Urlichs, D. Ondreka, K. Thoma, M. Kirk, and P. Spiller, "GSI electron lens for space charge compensation", in *Proc. IPAC'24*, Nashville, TN, USA, pp. 3186–3189, May 2024. doi:10.18429/JACoW-IPAC2024-THPC70

[13] N. Banerjee, J. A. Brandt, M. K. Duncan, Y. K. Kim, S. Nagaitsev, and G. Stancari, "Experiments on Electron Cooling and Intense Space-Charge at IOTA", in *Proc. COOL'23*, Montreux, Switzerland, pp. 114–119, Apr. 2024. doi:10.18429/JACoW-COOL2023-FRPAM1R3

[14] S. Nagaitsev, I. Lobach, E. G. Stern, and T. V. Zolkin, "McMillan electron lens in a system with space charge", *J. Instrum.*, vol. 16, no. 03, P03047, 2021. doi:10.1088/1748-0221/16/03/P03047

[15] S. Nagaitsev, V. V. Danilov, and A. Valishev, "Nonlinear Optics as a Path to High-Intensity Circular Machines", in *Proc. HB'10*, Morschach, Switzerland, Sep.-Oct. 2010, paper THO1D01, pp. 676–680.